TEMPERATURE ELEVATION OF A HUMAN BRAIN INDUCED BY A MOBILE PHONE ELECTROMAGNETIC RADIATION

***Uglješa Z. JOVANOVIĆ*[*1], *Dejan D. KRSTIĆ*[1], *Darko N. ZIGAR*[1], *Jelena R. MALENOVIĆ-NIKOLIĆ*[1], *Sveta G. CVETANOVIĆ*[1]**

[1]University of Niš, Faculty of Occupational Safety in Niš, Serbia

[*]Corresponding author; E-mail: ugljesa.jovanovic@znrfak.ni.ac.rs

This paper analyzes the specific absorption rate and the temperature elevation of the brain within an adult's man head exposed to electromagnetic radiation. The source of electromagnetic radiation is a contemporary mobile phone operating at 900 MHz. Simulations were performed on an anatomically accurate AustinMan 2.6 voxel-based human model with a resolution of 1x1x1 mm^3*. The thermal analysis focuses on temperature distribution on the brain surface in fixed time steps during one hour of continuous mobile phone use.*

Key words*: SAR, electromagnetic radiation, mobile phone, voxel-based human model, brain, temperature, simulation.*

1. Introduction

It is hard to imagine the modern way of life without mobile phones and their use. Their use inevitably imposes a growing number of long phone calls. However, mobile phones emit a low level of non-ionizing radiofrequency energy, a form of electromagnetic radiation (EMR) that all biological tissues can easily absorb. The massive use of mobile phones and the EMR they emit produce growing concern regarding the impact of EMR on human health. The concern grew since the International Agency for Research on Cancer (IARC) designated mobile phone EMR as Group 2B, possibly carcinogenic to humans [1].

The specific absorption rate (SAR) quantifies the absorption rate of EMR within all biological tissues. It refers to the amount of energy averaged over by a certain mass of biological tissues, i.e., 1 g or 10 g. There are two guidelines regarding exposure limits for mobile phone users in terms of SAR [2, 3]. Moreover, exposure to EMR mobile phones emit is regulated by prescribed maximal permissible levels for the head and limbs. In the USA, SAR is limited to 1.6 W/kg over 1 g of tissue [4], while in Europe, SAR is limited to 2 W/kg averaged over 10 g of tissue [5]. These values refer to the head and torso, while for limbs, SAR is limited to 4 W/kg. The noticeable effect of EMR on biological tissues is heating [6], i.e., while biological tissues absorb EMR, they heat up.

Many studies report that EMR emitted by mobile phones is partly absorbed by the brain due to proximity between them [6-8], which inevitably leads to the temperature increase of the brain [9, 10]. The temperature increase of the hypothalamus just by 0.2°C–0.3°C alters how the human body regulates its temperature [11, 12]. Moreover, reports suggest that EMR mobile phones emit can cause various neurological and cognitive disorders, such as headache, dizziness, memory loss, loss of concentration, and sleep disturbance [13-16]. Some studies suggest a relationship between EMR mobile phones emit and brain tumors [17-19].

The research presented in this paper analyzes the temperature elevation of the brain relative to the time when exposed to EMR emitted by a mobile phone at 900 MHz. Although there are many similar types of research, none provides temperature elevation of the brain in the time domain [10, 20, and 21].

2. Method and Modelling

Simulations presented in this research were performed using CST Studio, an electromagnetic simulating software based on the Finite Integration Technique (FIT) discretization of the integral form of Maxwell's equations [22].

The source of EMR in the presented research was a model of a contemporary smartphone available from CST Studio. The used mobile phone comprises properly organized components of any other contemporary smartphone, such as 2G, 3G, 4G, Wi-Fi antennas, a large LCD, battery, PCBs, camera, and plastic case. Although this mobile phone has four GSM antennas, only one emits notable EMR partly in the brain. Therefore, SAR distribution and thermal analysis were simulated only for this antenna, which operates in the 2G/3G band at 900 MHz.

The accuracy of SAR and temperature distribution inside a human head depends on the resolution of the employed human head model and the number of tissues it contains. A voxel-based model represents the anatomically realistic model of a human body, which is why they are highly used in various EMR simulations. Their main advantages are that they can easily map inhomogeneous tissues and have scalability. CST Studio offers HUGO, a voxel-based human model built from the Visible Human Male data set and designed explicitly for electromagnetic simulations. HUGO is 187 cm tall and 113 kg heavy, and it comprises 31 different tissues with a resolution of 1x1x1 mm^3. Numerous similar studies employ HUGO voxel-based model [23-25]. AustinMan 2.6 is the voxel-based human model, representing an improved version of the HUGO model, likewise used in many similar studies [26-30]. Although both share the exact resolution, AustinMan has 86 well-detailed tissues with improved boundaries between them compared to just 31 Hugo's. Good resolution and distinct boundaries between tissues are essential when many tissues are concerted in constricted space, such as the human head. Therefore, based on its well-established background, the AustinMan 2.6 voxel-based human model was used in the conducted simulations to obtain accurate results.

The scenario where the mobile phone was placed in a standard talking position was simulated. In other words, the mobile phone was leaned tightly against the right cheekbone of the AustinMan head. Fig. 1 shows the alignment between the head and mobile phone.

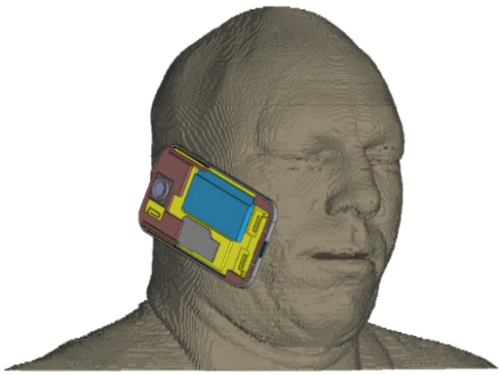

Fig. 1 Alignment between the head and mobile phone

The temperature of biological tissues is obtainable by solving Pennes' bioheat equation [31, 32], which can be expressed as:

$$\rho c \frac{\partial T}{\partial t} = \nabla(k \nabla T) - b(T - T_b) + q_{met} + \rho \mathrm{SAR} \quad (1)$$

The more common representation of blood perfusion heat-sink strength found in the literature is the blood perfusion rate. It relates to blood perfusion heat-sink strength via the following expression:

$$b = \rho \cdot \rho_{blood} \cdot m \cdot c_{blood} \cdot \frac{10^{-5}}{60} \quad (2)$$

Each biological tissue has dielectric and thermal properties necessary to calculate SAR and temperature distribution inside the head, so obtaining these values from good sources is essential. Dielectric properties are frequency-dependent, while thermal properties are not frequency-dependent. Dielectric and thermal parameters used in the presented research were sourced from the IT'IS foundation [33] and are given in Tab. 1.

Tab. 1. List of head tissues with their dielectric and thermal parameters at 900 MHz

Biological tissue	ε_r	σ	ρ	c	k	m	h
Blood Vessel	44.775	0.696	1102	3306	0.46	150	2.32
Bone Cortical	12.453	0.143	1908	1313	0.32	10	0.15
Bone Marrow	5.504	0.040	980	2065	0.19	30	0.46
Brain Grey Matter	52.725	0.942	1045	3696	0.55	764	15.54
Brain White Matter	38.886	0.590	1041	3583	0.48	212	4.32
Cartilage	42.652	0.782	1100	3568	0.49	35	0.54
Cerebellum	49.444	1.262	1045	3653	0.51	770	15.67
Cerebro Spinal Fluid	68.638	2.412	1007	4096	0.57	0	0
Dura	44.426	0.961	1174	3364	0.44	380	5.89
Eye Cornea	55.235	1.394	1062	3615	0.54	0	0
Eye Lens	46.572	0.793	1076	3133	0.43	0	0
Eye Sclera	55.270	1.166	1032	4200	0.58	380	5.89
Eye Vitreous Humor	68.901	1.636	1076	3133	0.43	0	0
Fat	5.461	0.051	911	2348	0.21	0	0
Lymph	59.683	1.038	1050	3609	0.52	5624	87.1
Medulla	49.444	1.262	1046	3630	0.51	559	11.37
Midbrain	49.444	1.262	1046	3630	0.51	559	11.37
Mucous Membrane	55.031	0.942	1102	3150	0.34	594	9.19
Muscle	55.031	0.942	1090	3421	0.49	37	0.91
Nerve	32.530	0.573	1075	3613	0.49	160	2.48
Pons	49.444	1.262	1046	3630	0.51	559	11.37
Salivary Gland	75.986	0.815	1048	3760	0.51	383	5.93
Skin	41.405	0.866	1109	3391	0.37	106	1.65
Spinal Cord	32.530	0.573	1075	3630	0.51	160	2.48
Tendon	45.825	0.718	1142	3432	0.47	29	0.45
Tongue	55.270	0.936	1090	3421	0.49	78	1.21

Tooth	12.453	0.143	2180	1255	0.59	0	0
Trachea	42.007	0.771	1080	3568	0.49	35	0.54

During simulations, in order to have comparative results, the reference power of the antenna was set to 1 W according to ICNIRP [2], IEEE standard [34], and other similar research [35-37]. The SAR distribution was obtained from the power loss density as a post-processing result according to the IEEE C95.3 standard averaging method over 1 g of tissue.

3. Simulation Results

Fig. 2 shows two curves, which help to analyze the depth of EMR absorption and temperature elevation of the brain. Both curves pass through the right temporal lobe, the area where the temperature elevation on the brain surface is the highest.

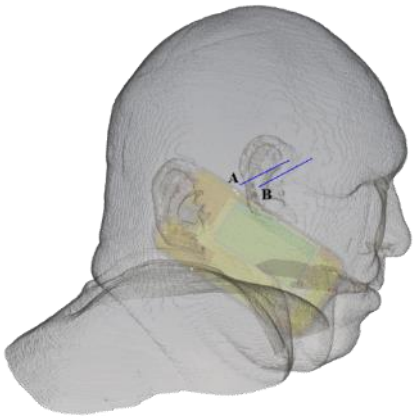

Fig. 2 Position of curves A and B

Curve B is directed to track the maximal temperature elevation inside the brain. Its starting position is in the center of the heat zone, where the highest temperature elevation is. The maximal temperature elevation area was traced via the brain's 1 mm long plot sections. Curve A serves as a control curve, and its role is to illustrate the heat penetration depth, and temperature elevation inside the heat zone. It is parallel to curve B and it lies just at the edge of the heat zone.

3.1. SAR_{1g} distribution

Fig. 3 shows the SAR_{1g} distribution on the surface of the head and for the horizontal cross-section in the region where the SAR_{1g} is at its highest peak.

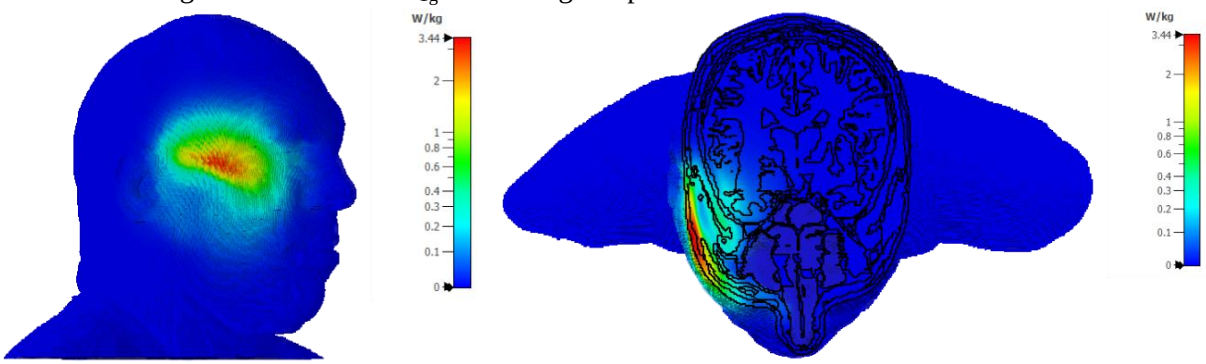

Fig. 3 SAR_{1g} distribution on the head surface

Fig. 3 shows that SAR_{1g} is concentrated on the entire right cheekbone and exceeds the maximal permissible value more than two times since the maximal value was 3.374 W/kg. The area colored red in Fig. 3 identifies the head tissues, which absorb the most energy. The SAR_{1g} is the highest within the skin and the fat tissue above the cheekbone. Moreover, SAR_{1g} is also present in the muscles, in the

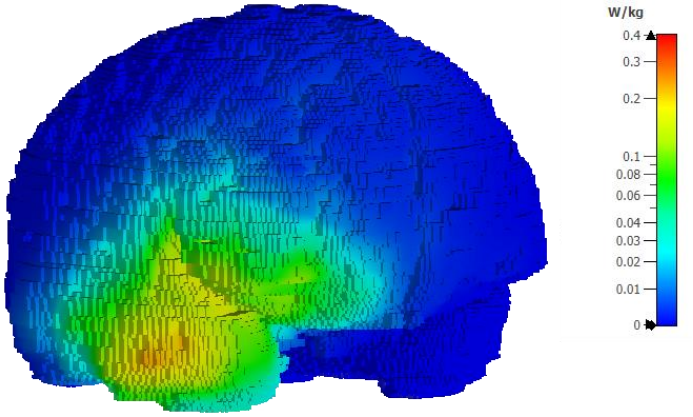

Fig. 4 SAR1g distribution on the brain surface

tendon and a small part of the EMR penetrates to the brain, where minimal SAR_{1g} values are still noticeable. Since the presented research focuses on the brain, Fig. 4 shows SAR_{1g} distribution on the brain surface, emphasizing the right temporal lobe.

As seen in Fig. 4, SAR_{1g} is concentrated on the entire right temporal lobe, where the maximal SAR_{1g} value was 0.242 W/kg. Based on figures 3 and 4, it is evident that SAR_{1g} rapidly decreases after being absorbed by the fat tissue. Such rapid drop can partly be associated with the antenna radiation pattern, which is not entirely directed towards the brain. Therefore, only a portion of the EMR reaches the brain.

3.2. Temperature distribution

Temperature distribution within the human head changes relative to the duration of the phone call. A dynamic thermal simulation was conducted for 60 minutes of straight mobile phone use to analyze this process thoroughly. Fig. 5 shows temperature distribution on the head surface in the initial state when no EMR was absorbed and after 60 minutes of straight mobile phone use as shown in Fig.

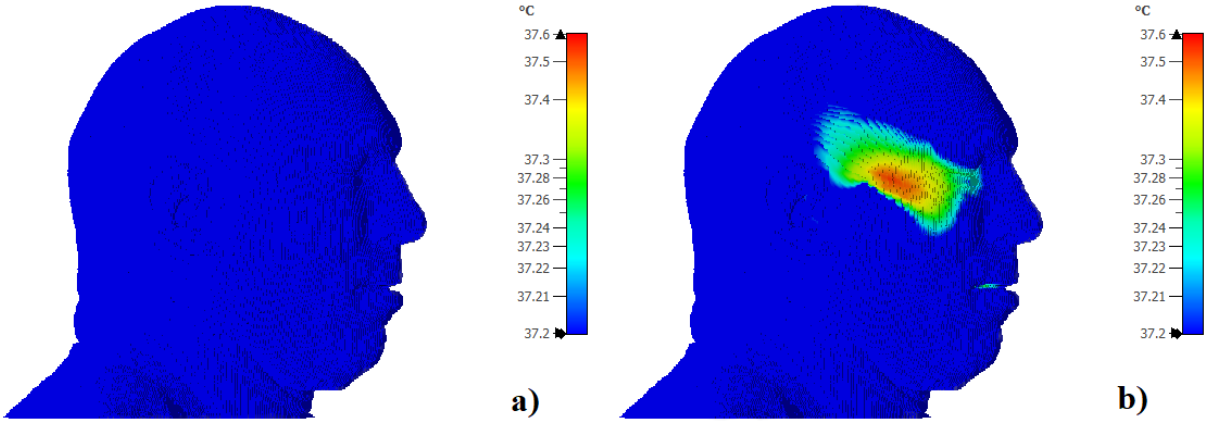

1.

Fig. 5 Temperature distribution on the head surface: a) in the initial state b) after 60 minutes of continuous phone call

In the initial state, the skin temperature is, as expected in the case of a healthy adult, less than 37.2°C. Namely, during this state, the maximal skin temperature was 37.0848°C, while the maximal skin temperature in the same zone after 60 minutes of straight mobile phone use was 37.5357°C. Consequently, the temperature difference between 60 minutes of the straight phone call and the initial state was exactly 0.4509°C. Fig. 6 shows temperature distribution on the brain surface before being exposed to the EMR. The temperature distribution shown in Fig. 6 will be the reference point for four measurement spots recorded every 15 minutes.

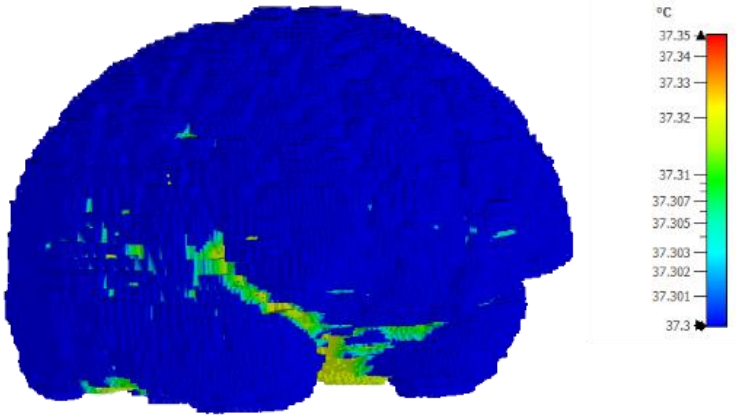

Fig. 6 Temperature distribution on the brain surface before the phone call

Since SAR_{1g} was concentrated on the right temporal lobe, it will inevitably heat up, which is why it is essential to identify the maximal temperature in this region, which was 37.2538°C. Fig. 7 shows temperature distribution on the brain surface after 15 minutes of continuous mobile phone use.

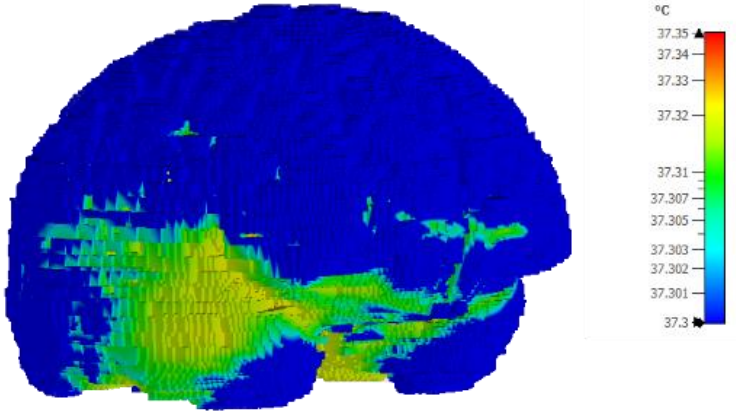

Fig. 7 Temperature distribution on the brain surface after 15 minutes of continuous phone call

As expected, Fig. 7 shows that a significant part of the right temporal lobe begins to heat up, and the maximal recorded temperature at this point was 37.3202°C. Consequently, the temperature difference between 15 minutes of the continuous phone call and the initial state is 0.0664°C. Fig. 8 shows temperature distribution on the brain surface after 30 minutes of continuous mobile phone use.

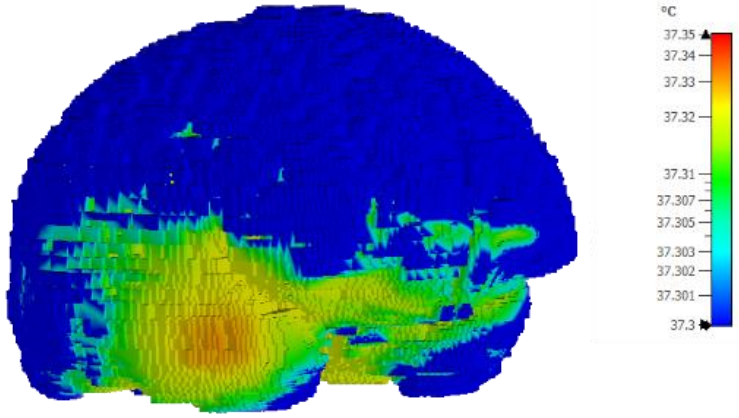

Fig. 8 Temperature distribution on the brain surface after 30 minutes of continuous phone call

After 30 minutes of continuous phone call heat area gradually expands, and the brain temperature increases. The maximal recorded temperature at this point was 37.3314°C, which is only 0.0776°C higher compared to the initial state when no phone call was conducted. Fig. 9 shows temperature distribution on the brain surface after 45 minutes of the continuous phone call.

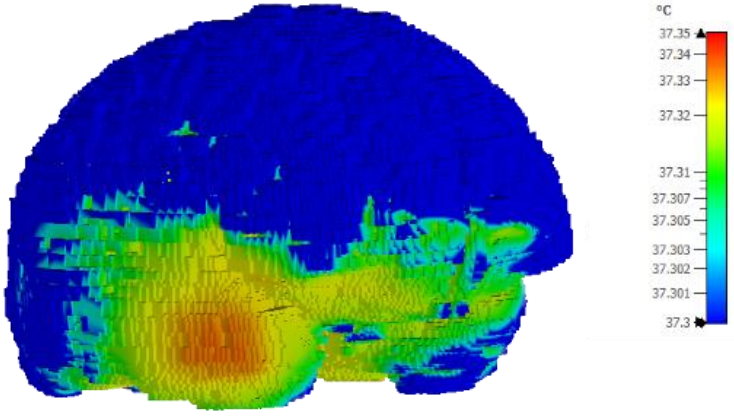

Fig. 9 Temperature distribution on the brain surface after 45 minutes of continuous phone call

A slight temperature increase is noticeable after 45 minutes of the continuous phone call, which also expands the heated area slightly. The maximal recorded temperature at this point was 37.3371°C, which means that the temperature elevation is 0.0833°C. Fig. 10 shows temperature distribution on the brain surface after 60 minutes of the continuous phone call.

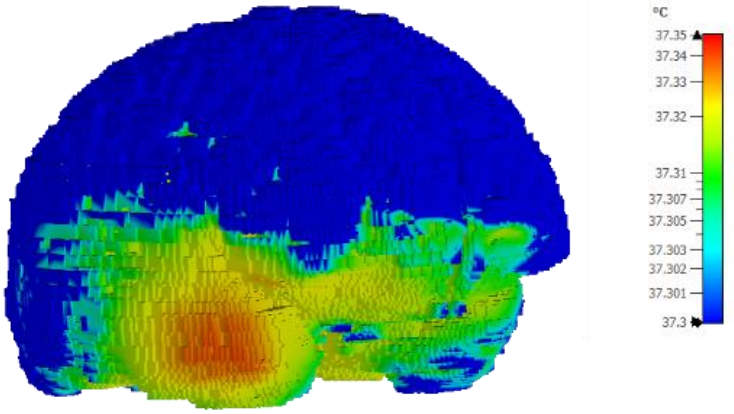

Fig. 10 Temperature distribution on the brain surface after 60 minutes of continuous phone call

Fig. 10 shows that after one hour of the continuous phone call, the maximal recorded temperature was 37.3415°C, which is only 0.0877°C higher compared to the initial state when no phone call is made.

Based on the previous results, it can be concluded that the temperature and heat gradually increase, and the difference between the initial state and 60 minutes of straight mobile phone use is less than 0.1°C, which means that blood flow keeps the brain sufficiently cool.

The antenna's output power significantly affects the temperature elevation in the brain. If the output power reduces, the temperature elevation will drop as well. Fig 11 shows temperature distribution on the brain surface after 60 minutes of the continuous phone call with 0.5 W of output power.

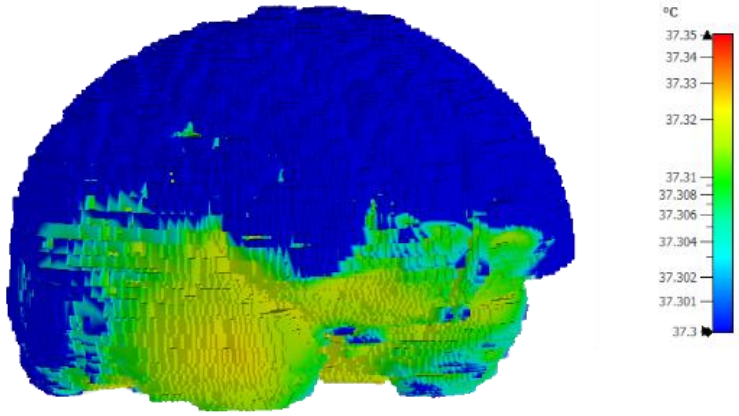

Fig. 11 Temperature distribution on the brain surface after 60 minutes with 0.5 W output power

The maximal recorded temperature on the brain surface when the antenna’s output power equals 0.5 W was 37.3243°C, corresponding to approximately 20 minutes of the continuous phone call when the antenna's output power was 1 W. Fig. 12 shows temperature distribution on the brain surface after 60 minutes of the continuous phone call when antenna’s output power is reduced to 0.25 W.

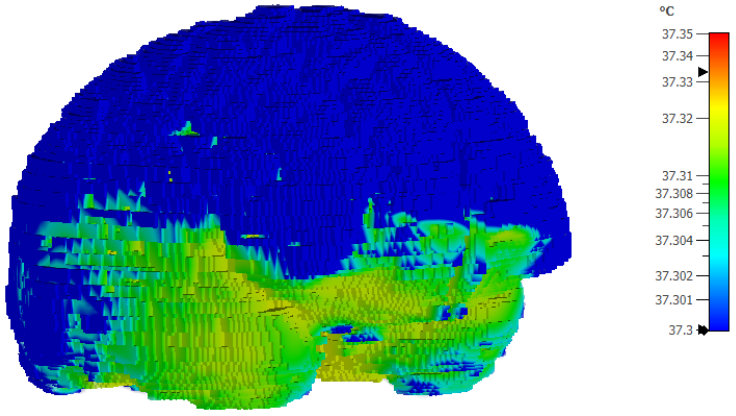

Fig. 12 Temperature distribution on the brain surface after 60 min. with 0.25 W output power

The maximal temperature in Fig. 12 was 37.3185°C, which corresponds to approximately 10 minutes of the continuous phone call when the antenna's output power was 1 W.

Curves A and B illustrate the depth of temperature elevation inside the brain. Fig. 13 shows comparative diagrams of temperature distribution along both curves inside the brain for the initial state and after 60 minutes of straight mobile phone use.

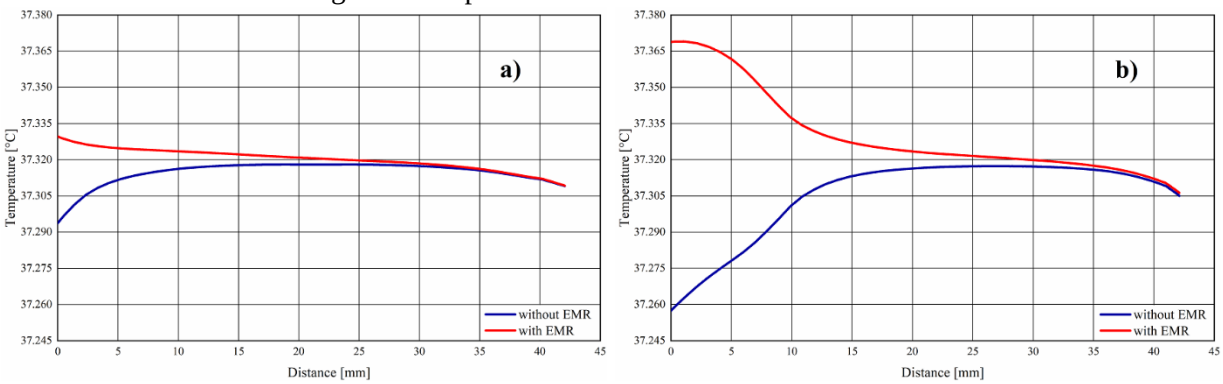

Fig. 13 Temperature distribution after 60 minutes of continuous phone call: a) along curve A; b) along curve B

Both diagrams show that at the point roughly 3 cm inside the brain, temperatures after 60 minutes of the straight call and when no phone call is made are almost identical because the difference between them is less than 0.001°C.

3.3. Comparison with similar research

Almost all mobile phones employ antennas with various positions and radiation patterns. Consequently, all mobile phones produce different SAR distributions and thermal effects [36]. Additionally, the position of the mobile phone has a significant role in temperature elevation.

Research [36], conducted using a diploe antenna, reports similar results whereby the maximal temperature elevation in the brain is 0.18°C. It should be noted that the dipole antenna has a significantly different radiation pattern compared to the one employed in this paper.

Although conducted on dead tissue, which is not cooled by the blood flow, the results presented in the research [38] are comparative with the results presented in this paper. Namely, the average brain temperature elevation after 10 minutes of continuous mobile phone use in research [38] was 0.1°C compared to 0.063°C recorded in the proposed research. Blood flow would lower the brain temperature, which is why the presented results are slightly lower.

Research [39] reports results similar to the results presented in this paper, where the maximum rise in brain temperature is 0.11°C. On the other hand, research [40] reports almost identical results to the results presented in this paper, where the maximal temperature elevation in the brain was 0.1°C.

4. Conclusion

Research presented in this paper analyses the SAR_{1g} distribution and temperature elevation of the human head in the time domain while it absorbs EMR emitted by a mobile phone. The emphasis of the research is particularly on temperature elevation of the brain.

An antenna with a partial radiation pattern directed to the brain was selected as the source of electromagnetic radiation. The anatomically accurate human head model with a sufficient number of tissues and resolution of 1x1x1 mm^3 was used to simulate EMR absorption and SAR and temperature distribution.

Because the mobile phone is leaned tightly against the head, the SAR_{1g} value is high and roughly exceeds the permissible level by twice. The obtained results demonstrate that one hour of continuous mobile phone usage increases the brain temperature roughly by 0.09°C in a 900 MHz band. The obtained results are in good correspondence with the results from the available literature.

Successful brain temperature maintenance can be attributed to the good thermal insulation of skin and fat and convective blood flow. Based on these results, it can be concluded that mobile phone EMR produces a minimal effect on the brain, even after a phone call for as long as one hour. Consequently, brain function is slightly impacted by the absorbed EMR. However, to minimize brain heating, a mobile phone user can frequently toggle the mobile phone position between one ear and another, thus allowing the blood flow to cool down the heated tissues and one side of the brain.

It should be noted that mobile phones have different antenna positions and radiation patterns, producing different results, some of which may have significantly higher brain temperature elevation.

Acknowledgment

The presented research has been funded by the Ministry of Education, Science, and Technological Development of the Republic of Serbia.

Nomenclature

b – heat-sink strength from each tissue volume by blood perfusion [Wm^3-1°C-1]
c – tissue specific heat capacity [Jkg-1°C -1]
c_{blood} – specific heat capacity of blood [Jkg-1°C -1]
ε_r – tissue permittivity [Fm-1]
h – tissue heat generation rate [Wkg-1]
k – tissue thermal conductivity [Wm-1°C-1]
m – blood perfusion rate [ml-1min-100 g-1]
q_{met} – tissue metabolic heat generation [Wm^3-1]
ρ – tissue mass density [kgm^3-1]
ρ_{blood} – mass density of blood [kgm^3-1]
σ – tissue conductivity [Sm-1]
T – tissue temperature [°C]
T_b – blood temperature [°C]

References

[1] Baan R., *et al*., Carcinogenicity of radiofrequency electromagnetic fields, *The Lancet Oncology*, 12.7 (2011), pp. 624–626

[2] International Commission on Non-Ionizing Radiation Protection, ICNIRP statement on the guidelines for limiting exposure to time-varying electric, magnetic, and electromagnetic fields (up to 300 GHz), *Health Physics*, 97.3 (2009), pp. 257–259

[3] IEEE C95.1-2019, IEEE Standard for Safety Levels with Respect to Human Exposure to Electric, Magnetic, and Electromagnetic Fields, 0 Hz to 300 GHz, 2019

[4] Federal Communications Commission, Specific absorption rate (SAR) for cellular telephones, 2012

[5] IEC International Electrotechnical Commission, Human Exposure to Radio Frequency Fields from Hand-Held and Body-Mounted Wireless Communication Devices–Human Models, Instrumentation, and Procedures to Determine the Specific Absorption Rate (SAR) for Hand-Held Devices Used in Close Proximity to the Ear (Frequency Range of 300MHz to 3 GHz), 2005

[6] Huber R., *et al.*, Radio frequency electromagnetic field exposure in humans: Estimation of SAR distribution in the brain, effects on sleep and heart rate, *Bioelectromagnetics*, 24.4 (2003), pp. 262-276.

[7] Kim, J. H., *et al.*, Possible effects of radiofrequency electromagnetic field exposure on central nerve system, *Biomolecules & Therapeutics*, 27.3 (2019), pp. 265–275

[8] Hu, C., *et al.*, Effects of radiofrequency electromagnetic radiation on neurotransmitters in the brain, *Frontiers in Public Health*, 9 (2021), no. 691880

[9] Van Den Berg, P. M., *et al.*, A computational model of the electromagnetic heating of biological tissue with application to hyperthermic cancer therapy, *IEEE Transactions on Biomedical Engineering*, 12 (1983), pp. 797-805

[10] Stanković, V., *et al.*, Temperature distribution and specific absorption rate inside a child's head, *International Journal of Heat and Mass Transfer*, 104 (2017), pp 559-565

[11] Adair, E. R., *et al.*, Minimal changes in hypothalamic temperature accompany microwave-induced alteration of thermoregulatory behavior, *Bioelectromagnetics*, 5.1 (1984), pp. 13-30.

[12] Tan, C. L., *et al.*, Regulation of body temperature by the nervous system, *Neuron*, 98.1 (2018), pp. 31-48

[13] Frey, A. H., Headaches from cellular telephones: are they real and what are the implications?, *Environmental Health Perspectives*, 106.3 (1998), pp. 101-103.

[14] Danker-Hopfe, H., *et al.*, Effects of mobile phone exposure (GSM 900 and WCDMA/UMTS) on polysomnography based sleep quality: An intra-and inter-individual perspective, *Environmental Research*, 145 (2016), pp. 50-60

[15] Hutter, H. P., *et al.*, Subjective symptoms, sleeping problems, and cognitive performance in subjects living near mobile phone base stations, *Occupational and Environmental Medicine*, 63.5 (2006), pp. 307-313

[16] Abdel-Rassoul, G., *et al.*, Neurobehavioral effects among inhabitants around mobile phone base stations, *Neurotoxicology*, 28.2 (2007), pp. 434-440

[17] Swerdlow, A. J., *et al.*, Mobile phones, brain tumors, and the interphone study: where are we now?, *Environmental Health Perspectives*, 119.11 (2011), pp. 1534-1538

[18] Repacholi, M. H., *et al.*, Systematic review of wireless phone use and brain cancer and other head tumors, *Bioelectromagnetics*, 33.3 (2012), pp. 187-206

[19] Morgan, L. L., *et al.*, Mobile phone radiation causes brain tumors and should be classified as a probable human carcinogen (2A), *International Journal of Oncology*, 46.5 (2015), pp. 1865-1871

[20] Kodera, S., *et al.*, Temperature elevation in the human brain and skin with thermoregulation during exposure to RF energy, *Biomedical Engineering Online*, 17.1 (2018), pp 1-17

[21] Kaburcuk, F., Elsherbeni, A. Z., Efficient computation of SAR and temperature rise distributions in a human head at wide range of frequencies due to 5G RF field exposure, *The Applied Computational Electromagnetics Society Journal (ACES)*, 33.11 (2018), pp. 1236-1242

[22] Weiland, T., A discretization model for the solution of Maxwell's equations for six-component fields, *Archiv Elektronik und Uebertragungstechnik*, 31 (1977), pp. 116-120

[23] Barchanski, A., et al., Local grid refinement for low-frequency current computations in 3-D human anatomy models, *IEEE Transactions on Magnetics*, 42.4 (2006), pp. 1371-1374

[24] Barchanski, A., *et al.*, Large-scale calculation of low-frequency-induced currents in high-resolution human body models, *IEEE Transactions on Magnetics*, 43.4 (2007), pp. 1693-1696

[25] Arif, A., *et al.*, A compact, low-profile fractal antenna for wearable on-body WBAN applications, *IEEE Antennas and Wireless Propagation Letters*, 18.5 (2019), pp. 981-985

[26] Massey, J. W. Yılmaz, A. E., AustinMan and AustinWoman: High-fidelity, anatomical voxel models developed from the VHP color images, in Proc. 38th Annu. Int. Conf. IEEE Eng. Med. Biol. Soc., Orlando, FL, (2016), pp. 3346–3349

[27] Fujimoto, K., *et al.*, Radio-frequency safety assessment of stents in blood vessels during magnetic resonance imaging, *Frontiers in Physiology*, 9 (2018): 1439.

[28] Wagih, M., *et al.*, Dual-band dual-mode textile antenna/rectenna for simultaneous wireless information and power transfer (SWIPT), *IEEE Transactions on Antennas and Propagation*, 69.10 (2021), pp. 6322-6332

[29] Bisio, I., *et al*. Brain stroke microwave imaging by means of a Newton-conjugate-gradient method in Lp banach spaces, *IEEE Transactions on Microwave Theory and Techniques*, 66.8 (2018), pp. 3668-3682.

[30] Kaim, V., *et al*., Ultra-miniature circularly polarized CPW-fed implantable antenna design and its validation for biotelemetry applications, *Scientific Reports*, 10.1 (2020), pp. 1-16

[31] Pennes, H. H., Analysis of tissue and arterial blood temperatures in the resting human forearm, *Journal of Applied Physiology*, 1.2 (1948), pp. 93-122

[32] McIntosh, R. L., Anderson, V., A comprehensive tissue properties database provided for the thermal assessment of a human at rest, *Biophysical Reviews and Letters*, 5.03 (2010), pp. 129-151

[33] Hasgall, P. A., *et al.*, IT'IS Database for thermal and electromagnetic parameters of biological tissues, Version 4.1, 2022

[34] IEC/IEEE 62704-4, International standard, 2020

[35] Beard B., *et al.*, Comparisons of computed mobile phone induced SAR in the SAM phantom to that in anatomically correct models of the human head, *IEEE Transactions on Electromagnetic Compatibility*, 48.2 (2006), pp. 397-407

[36] Kodera, S., *et al.*, Temperature elevation in the human brain and skin with thermoregulation during exposure to RF energy, *Biomedical Engineering Online*, 17.1 (2018), pp. 1-17

[37] Wessapan, T., *et al.*, Specific absorption rate and temperature distributions in human head subjected to mobile phone radiation at different frequencies, *International Journal of Heat and Mass Transfer*, 55.1-3 (2012), pp. 347-359

[38] Christopher, B., *et al.*, Empirical study on specific absorption rate of head tissues due to induced heating of 4G cell phone radiation, *Radiation Physics and Chemistry*, 178 (2021), p.n. 108910

[39] Van Leeuwen, G. M. J., *et al*., Calculation of change in brain temperatures due to exposure to a mobile phone, *Physics in Medicine & Biology*, 44.10 (1999), pp. 2367-2378

[40] Fujimoto, M., *et al.*, FDTD-derived correlation of maximum temperature increase and peak SAR in child and adult head models due to dipole antenna, *IEEE Transactions on Electromagnetic Compatibility*, 48.1 (2006), pp. 240-247

Submitted: 18.07.2022.

Revised: 24.09.2022.

Accepted: 04.10.2022.